ACS APPLIED MATERIALS & INTERFACES

Research Article

www.acsami.org

Pure and Stable Top-Emitting White Organic Light-Emitting Diodes Utilizing Heterojunction Blue Emission Layers and Wide-Angle Interference

Lingling Deng,[†,§] Hongying Shi,[†,§] Xue Meng,[†,∥] Shufen Chen,*[,†] Hongwei Zhou,[†] Ying Xu,[†] Xingao Li,[†] Lianhui Wang,[†] Bin Liu,[†] and Wei Huang*[,†,‡]

[†]Key Laboratory for Organic Electronics and Information Displays and Institute of Advanced Materials, Nanjing University of Posts and Telecommunications, Nanjing 210023, China

[‡]Jiangsu-Singapore Joint Research Center for Organic/Bio-Electronics & Information Displays and Institute of Advanced Materials, Nanjing Tech University, Nanjing 211816, China

ABSTRACT: In top-emitting white organic light-emitting diodes (TWOLEDs), it is usually difficult to realize a good chromaticity due to the strong suppression on the blue emission induced by the microcavity effect. In our work, the blue emission layer (EML) is located near the hole transport layer and the reflective anode to strengthen the wide-angle interference on the blue emission and enhance the output of light. Then we utilize the dual blue EMLs based on an electron-rich heterojunction to constrain most of the excitons in the blue EMLs. With the above two strategies, the intensity of the blue emission is significantly enhanced accompanying the chromaticity improvement in white emission. Some key factors including exciton distribution, energy transfer, and carrier trapping are analyzed to design the structure of the EMLs to acquire the pure and stable white emission. The excellent color stability with a Commission International de L'Eclairage (CIE) coordinate drift of only (0.009, 0.001) in the luminance range of 10−10^4 cd/m^2 is obtained in our optimized TWOLED. The TWOLED also shows the high performances with a maximum luminance of 15360 cd/m^2, the CIE coordinates of (0.33, 0.41), and a current efficiency of 13.3 cd/A.

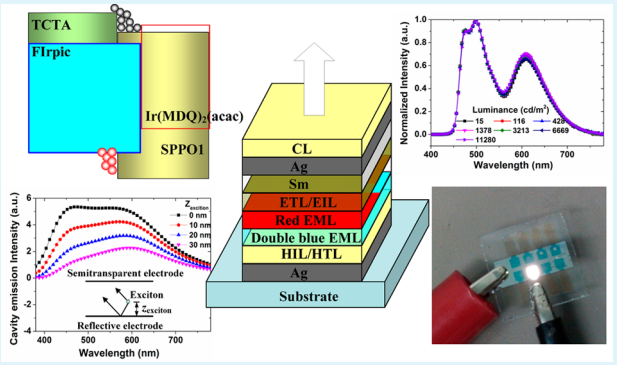

KEYWORDS: *organic light-emitting diode, top-emitting, white, stability, dual blue emission layer, heterojunction, wide-angle interference*

INTRODUCTION

Since the first white organic light-emitting diode (WOLED) was realized by Kido and his co-workers, WOLEDs have attracted considerable attention due to their potential application in flat-panel displays and solid-state lighting and made tremendous progress.[1,2] Top-emitting WOLEDs (TWOLEDs), emitting light through a transparent or semitransparent top electrode, can be deposited onto any substrates including flexible substrates such as metal foils and plastics and are better suited for active-matrix application.[3,4] To meet the commercial application demand, WOLEDs should possess not only high performances such as brightness, efficiency, and lifetime but also better chromatic properties such as the Commission International de L'Eclairage (CIE) chromaticity coordinates of near (0.33, 0.33), a correlated color temperature (CCT) of between 2500 and 6500 K, a color-rendering index (CRI) of above 80, and the color stability of CIE coordinates drift under (0.01, 0.01) in the whole brightness range.[5] Unfortunately, it is difficult to realize both high performances and better chromatic properties in TWOLEDs.[6−9]

In TWOLEDs, metals are usually utilized as both the anode and the cathode due to their better conductivity and uncomplicated preparation technique. However, their low work function will obstruct the injection of holes, increase the operation voltage, and result in the carrier imbalance when metals are used as the anodes. On the other hand, when metals are utilized as the reflective anode and the semitransparent cathode, the microcavity effect usually occurs due to their high reflectivities, which decreases the output of light and makes the emission spectra deviate from a standard white spectrum.[10] The design of the reflectivity of the electrodes is the most commonly used method to improve the performances of the TWOLEDs, e.g., metal/dielectric based anode or cathode,[11,12] bilayer electrodes,[13,14] carbon nanotube cathode,[3] and out-coupling layers.[15−17] By reducing the reflectivity of the electrode, the multibeam interference in the microcavity is effectively suppressed, and the output is enhanced. In addition

Received: January 28, 2014
Accepted: March 12, 2014
Published: March 12, 2014

   dx.doi.org/10.1021/am5006354 | *ACS Appl. Mater. Interfaces* 2014, 6, 5273−5280

to the multibeam interference, the wide-angle interference relying on the position of the emission excitons in the microcavity is also an important factor restraining the device performances. When the multibeam interference is weak, the wide-angle interference greatly influences the microcavity effect, so the position of the excitons can be adjusted to further improve the light output.[18,19] However, there are only a few studies focusing on the enhanced wide-angle interference in monochromic or white OLEDs because changing the exciton position will influence not only the optical but also the electrical properties of the devices, which is relatively difficult to design.[15,20]

In this work, the position of excitons is first discussed to strengthen the microcavity resonance on the blue light by a homemade optical simulation procedure, and then the dual blue emission layer (EML) structure based on a heterojunction is utilized to control the exciton position to realize the emission enhancement on the blue light. Finally, the structure of the TWOLED is optimized by analyzing the various kinds of working mechanisms, including the carrier transport, the exciton diffusion, the energy transfer, and the charge trapping. The optimized TWOLED simultaneously exhibits a high efficiency, a pure chromaticity, and an excellent color stability.

OPTICAL AND ELECTRICAL DESIGN

Wide-Angle Interference. A top-emitting organic light-emitting diode (TOLED) consists of a reflective anode, a semitransparent cathode, and several organic layers sandwiched in between. The microcavity effect, including multibeam interference and wide-angle interference, exists in the TOLED due to the high reflectance of both the anode and the cathode. Usually, multibeam interference is the main resonance mechanism in the microcavity, relying on the reflectivities of the electrodes and the total thickness of the organic layers. Once the reflectivity of the semitransparent cathode reduces, the multibeam interference becomes weak, and the resonance in the microcavity greatly correlates with the wide-angle interference. The resonant wavelength of the wide-angle interference is determined by

$$-|\phi_B| + \frac{4\pi z_E}{\lambda} = m2\pi \quad (1)$$

Here, ϕ_B is the phase change on reflectance of the reflective anode; z_E is the optical length between the emission exciton and the reflective anode; λ is the resonant wavelength; and m is the resonance mode number. From eq 1, the resonant wavelength exhibits a blue shift with the decrease of z_E, which is facilitated to enhance the intensity of the blue emission.[21] For a multilayer TOLED, we calculate the cavity emission spectra with a classic electromagnetic model,[21] as shown in Figure 1. The TOLED structure is of glass substrate/Ag (80 nm)/hole transport layer (HTL, 35 nm)/EML (30 nm, $z_{exciton}$)/electron transport layer (ETL, 35 nm)/Sm (4 nm)/Ag (12 nm)/coupling layer (CL 40 nm). Here, the HTL is composed of 4,4′,4″-tris(3-methylphenylphenylamino) triphenylamine (*m*-MTDATA, 25 nm) and *N*,*N*′-di(naphthalene-1-yl)-*N*,*N*′-diphenyl-benzidine (NPB, 10 nm); the ETL is 4,7-diphenyl-1,10-phenanthroline (BPhen); the EML consists of 4,4′-bis(carbazol-9-yl)-biphenyl (CBP) and some emission guest materials; and the CL is *m*-MTDATA. $z_{exciton}$ is the physical length between the exciton and the EML/HTL interface, which will be varied to study the wide-angle interference. In the calculation, the complex refractive indices

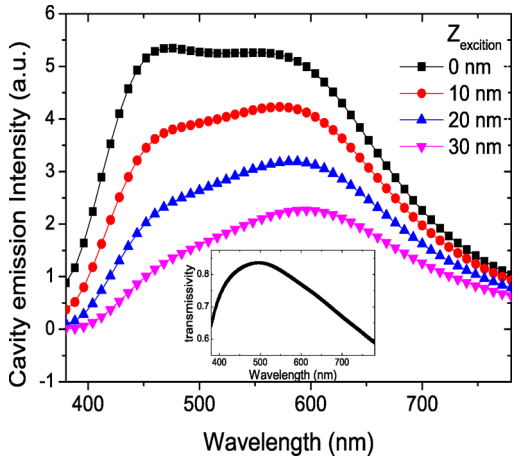

Figure 1. Cavity emission spectra of the TOLEDs with different exciton positions. Inset is the calculated transmissivity of the semitransparent cathode.

of all the materials are measured with an M-2000UI Ellipsometer. For the calculation of the cavity emission spectra in Figure 1, it is only considered of microcavity with all emissive materials being ignored.

By utilizing the double-layer cathode structure and the coupling layer, the optimized semitransparent cathode has a high transmissivity of above 0.82 in the blue emission band as shown in the inset of Figure 1. Thus, the suppression on the blue emission induced by the multibeam interference is greatly reduced. From Figure 1, the cavity emission intensity which means the resonance intensity induced by the microcavity increases with the decrease of $z_{exciton}$ in the whole visible wavelength range. In addition, the resonance enhancement on the blue emission band is more obvious than that on the red band. The peak of the cavity emission spectrum is around 600 nm when the emission excitons locate near the EML/ETL interface ($z_{exciton}$ = 30 nm), while it shifts to around 465 nm with $z_{exciton}$ = 0 nm. So it is facilitated to enhance the output of blue emission and to acquire the balance white light when a blue phosphor is incorporated into the EML close to the reflective anode.

Carrier Transport. To further realize the wide-angle interference enhancement on the blue emission, we plan to introduce a heterojunction into the EML to control the exciton position. Here, 4,4′,4″-tris(*N*-carbazolyl)-triphenylamine (TCTA) is used as the hole-transport matrix material, and 2-(diphenylphosphoryl)spirofluorene (SPPO1) is used as the electron-transport host material. Energy differences of 0.8 eV between the highest occupied molecular orbitals (HOMOs) and 0.4 eV between the lowest unoccupied molecular orbitals (LUMOs) of TCTA and SPPO1 provide the hole and electron barriers. In such a heterojunction EML, the interface of TCTA/SPPO1 is the main exciton formation zone.[22] Besides, both materials provide high triplet levels with energies of approximately 2.8 eV.

We use iridium(III) bis[(4,6-difluorophenyl)-pyridinato-N,C$^{2'}$] picolinate (FIrpic) and iridium(III) bis(2-methyldibenzo[f,h]quinoxaline)(acetylacetonate) [Ir(MDQ)$_2$(acac)] as blue and red phosphor guests. In a host–guest system, guest molecules may serve as the transport channels or carrier trap sites, which finally influences the carrier transport and exciton formation zone in the devices.[23] Some single-carrier devices are fabricated to study the hole and

dx.doi.org/10.1021/am5006354 | ACS Appl. Mater. Interfaces 2014, 6, 5273–5280

electron behaviors of the two kinds of guests and guide the design of the EML structure. We fabricate two groups of single-carrier devices, based on TCTA and SPPO1 host material, respectively. The structures are of Ag (80 nm)/MoO_x (2 nm)/*m*-MTDATA (25 nm)/NPB (10 nm)/EML (30 nm)/NPB (10 nm)/*m*-MTDATA (25 nm)/MoO_x (2 nm)/Ag (15 nm) for hole-only and Ag (80 nm)/Sm (4 nm)/BPhen (35 nm)/EML (30 nm)/BPhen (35 nm)/Sm (4 nm)/Ag (15 nm) for electron-only devices. Here, TCTA, TCTA:7 wt % FIrpic, SPPO1, SPPO1:7 wt % FIrpic, and SPPO1:4 wt % $Ir(MDQ)_2(acac)$ are used as EMLs, respectively. From Figure 2a, devices with FIrpic-doped EMLs present the larger hole-

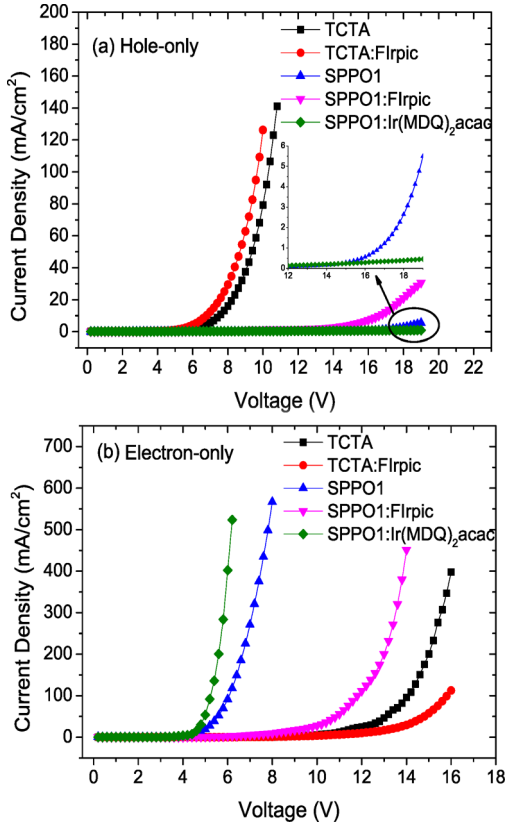

Figure 2. Current density–voltage characteristics of hole-only (a) and electron-only (b) devices.

current density than the undoped ones, indicating FIrpic molecules act as the hole-transport channel in TCTA and SPPO1. In contrast, the electron current is reduced due to the doping of FIrpic, showing that the electrons are trapped by FIrpic molecules in TCTA and SPPO1 (Figure 2b). Similarly, according to the current density of single-carrier devices doped and undoped $Ir(MDQ)_2(acac)$, we can determine that the $Ir(MDQ)_2(acac)$ molecule serves as the electron-transport channel and the hole trap in SPPO1. So more holes and electrons will accumulate at the TCTA/SPPO1 interface and form excitons when FIrpic is doped in TCTA and $Ir(MDQ)_2(acac)$ is doped in SPPO1, which facilitates the high efficiency.

Basic Structure of the Emission Layers. On the basis of the above analysis on the wide-angle interference and carrier transport in the TWOLED, the dual blue EMLs with the structure of TCTA:7 wt % FIrpic/SPPO1:7 wt % FIrpic are introduced to acquire sufficient blue emission. $Ir(MDQ)_2(acac)$ is doped with concentration of 4 wt % into SPPO1 next to FIrpic as the red emitter. The energy levels of the EMLs and the chemical structures of the materials used are shown in Figure 3, and the HOMOs and LUMOs of the used host and guest molecules are also presented. The blue EMLs are located near the reflective anode to realize the enhanced microcavity resonance on the blue emission band. At the same time, the hole channel provided by FIrpic molecules in TCTA and the electron channel provided by $Ir(MDQ)_2(acac)$ molecules in SPPO1 increase the number of carriers reaching the interface. The excitons are formed at the TCTA/SPPO1 interface and then diffuse into the TCTA and SPPO1 layers. The thickness of the second blue EML (SPPO1:7 wt % FIrpic) greatly affects the exciton proportion in the blue and red EMLs, so it should be adjusted to acquire a pure and stable white emission.

EXPERIMENTAL SECTION

The TWOLEDs were fabricated on the precleaned glass substrates. All organic layers and metal layers were deposited by thermal evaporation with a deposition rate of 0.1–0.2 nm/s in a high vacuum about 5×10^{-4} Pa without breaking the vacuum. For the case of doping, the deposition rates of both host and guest were controlled with their correspondingly independent quartz crystal oscillators. The current–voltage–luminance and the spectra characteristics are measured by the recombination of a Keithley 2400 source measurement unit with a Photo-Research-655 Spectroscan Colorimeter in room-temperature nitrogen gas.

The transient photoluminescence (PL) measurements were carried out using a steady-state and time-resolved fluorescence/phosphorescence spectrometer (FLSP920). A microsecond flashlamp was used as the photoexcitation source.

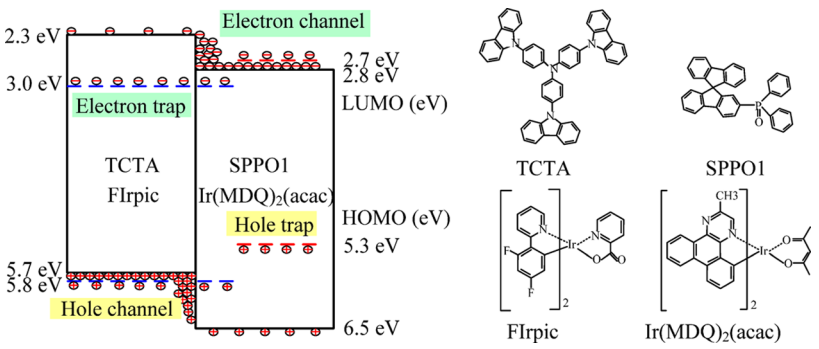

Figure 3. Energy levels and chemical structures of the materials used in the emission layers.

dx.doi.org/10.1021/am5006354 | ACS Appl. Mater. Interfaces 2014, 6, 5273–5280

RESULTS AND ANALYSIS

Exciton Distribution. To analyze the exciton distribution in SPPO1 near the TCTA/SPPO1 interface, we fabricate a group of devices owning a blue emission layer of 1 nm at different places in the SPPO1 layer. The EML structures of the four devices are: TCTA (15 nm)/SPPO1 (x nm)/SPPO1:7 wt % FIrpic (1 nm)/SPPO1 ($14 - x$ nm), where x = 1, 5, 9, and 13. The structures of the carrier transport layers and the electrodes are the same as those in the microcavity calculation. In Figure 4a, the measured luminance and the fitted curves are presented. We assume that all radiations originate from the excitons in the EML, and the luminance is proportional to the concentration of the excitons. Excitons, generated at the TCTA/SPPO1 interface, will diffuse into SPPO1, reaching a steady state of exponentially decaying distribution with characteristic width L_D.[24] We fit the exciton distribution with an exponential function. We find the diffusion lengths are 5.2, 5.2, and 5.3 nm at 4, 5, and 6 V, respectively, which keeps almost unchanged because only a few holes are injected into SPPO1 and the excitons accumulate near the TCTA/SPPO1 interface in the case of the low voltage. When the voltage increases to 7 V, more holes acquire sufficient energy to cover the barrier, so more excitons are formed and diffuse into SPPO1, resulting in the increase of the diffusion length. The change of L_D shows that the exciton recombination zone is becoming wider slowly with the increased voltage.

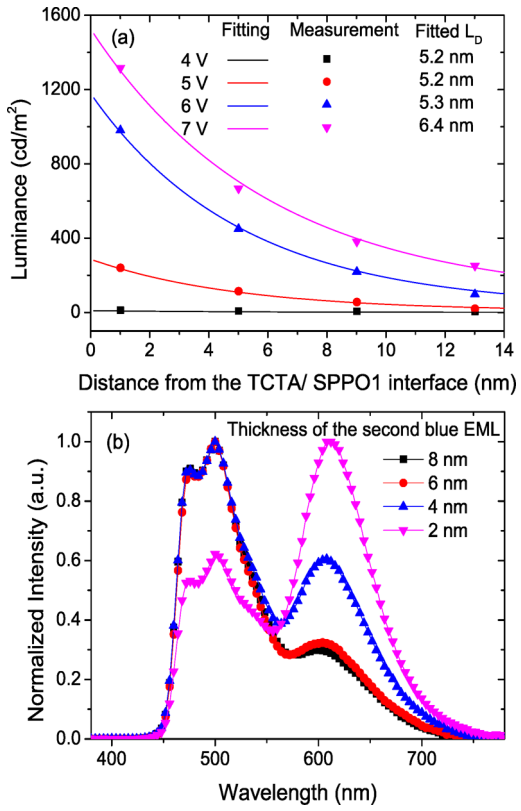

Figure 4. (a) Luminance of the devices with a thin blue emission layer at different places in SPPO1. (b) Normalized spectra of TWOLEDs with the different thicknesses of the second blue EML.

We make four white devices with EMLs of TCTA:7 wt % FIrpic (15 nm)/SPPO1:7 wt % FIrpic (y nm)/SPPO1:4 wt % Ir(MDQ)$_2$(acac) ($15 - y$ nm) to further test the main exciton distribution distance from the TCTA/SPPO1 interface, where y = 8, 6, 4, and 2. As shown from the curves of 8 and 6 nm in Figure 4b, the red part in the white spectra is very weak because the red EML locates out of the diffusion length of 5−6 nm. With the red EML closing to the TCTA/SPPO1 interface, the intensity of red emission is significantly enhanced. When it is very close to the interface, the red part dominates the generated white emission (shown as the curve of 2 nm). The TWOLED with a second blue EML (SPPO1:7 wt % FIrpic) of 4 nm shows a very pure white spectrum due to the relatively strong blue emission.

Energy Transfer Processes. In a host−guest doping system, the energy transfer from the host to the guest molecules is the dominate emission process. In our TWOLEDs, triplet excitons are first formed on the TCTA and SPPO1 molecules and then are transferred to the FIrpic and Ir(MDQ)$_2$(acac) ones, which finally generate the blue and red emission. Besides, energy transfer from the FIrpic to Ir(MDQ)$_2$(acac) molecules also influences the intensity of the two kinds of emission and the chromaticity of the white light. To investigate the energy transfer process between the two emitters, we fabricate three devices I1−I3 with different EML structures of TCTA:7 wt % FIrpic (15 nm)/SPPO1:7 wt % FIrpic ($4 - z$ nm)/SPPO1 (z nm)/SPPO1:4 wt % Ir(MDQ)$_2$(acac) (11 nm), where SPPO1 acts as the interlayer, and z = 0, 1, and 2 for devices I1 to I3. It is noted that the carrier transport layers and the electrodes in devices I1−I3 are still the same with the aforementioned devices. In this group of devices, the thickness of the second blue EML decreases along with the increase of the interlayer, and the red EML thickness remains unchanged. As shown in Figure 5a, the device I1 shows the weakest blue emission, although it has the thickest blue EML, while the red emission from device I1 is the strongest among the three devices. The reason is that there exists obvious energy transfer from the blue to the red emitters due to the absence of the interlayer. In device I2, the energy transfer is partly suppressed by using a 1 nm interlayer, which can be seen from the decrease of the red emission and the increase of the blue emission compared to those in device I1. When the interlayer thickness increases to 2 nm (device I3), the energy transfer is almost completely suppressed.

Furthermore, the ratios of blue and red parts in the white spectra at different currents are studied in devices I1−I3. We calculate the resolved spectra of the two emitters and then derive their relative ratio according to the method given in the literature,[22] and the results are presented in Figure 5b. We find that the contribution of the blue emitter increases, while the red contribution decreases with the interlayer thickness increasing at any current, showing the stable energy transfer process between the two emitters. Additionally, device I1 displays a more stable ratio than the other two devices, which demonstrates that it is helpful to improve the color stability by strengthening the energy transfer between the different emitters in our TWOLEDs.

The energy transfer process between two phosphors includes the Förster process and Dexter process. The former has a larger transfer radius (4−5 nm) than the latter (1−2 nm).[25,26] As shown in Figure 5a, the energy transfer is greatly suppressed when the thickness of the interlayer exceeds 1 nm, which means the Dexter process mainly contributes to the energy transfer from FIrpic to Ir(MDQ)$_2$(acac) molecules. The transient PL decay curves of SPPO1:7 wt % FIrpic layer (3 nm) (sample 1) and SPPO1:7 wt % FIrpic (3 nm)/SPPO1:4 wt % Ir(MDQ)$_2$(acac) (3 nm) layers (sample 2) are presented in

dx.doi.org/10.1021/am5006354 | ACS Appl. Mater. Interfaces 2014, 6, 5273−5280

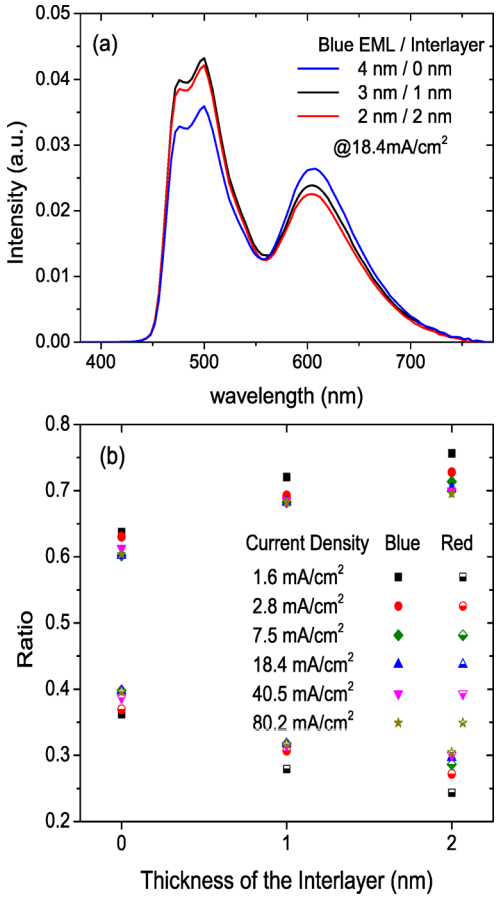

Figure 5. Spectra (a) and ratios of the blue and red parts in the spectra (b) of the devices with the different second blue EMLs and interlayers.

Figure 6. We observe that the PL intensity at 474 nm decays faster due to the presence of the SPPO1:4 wt % Ir-

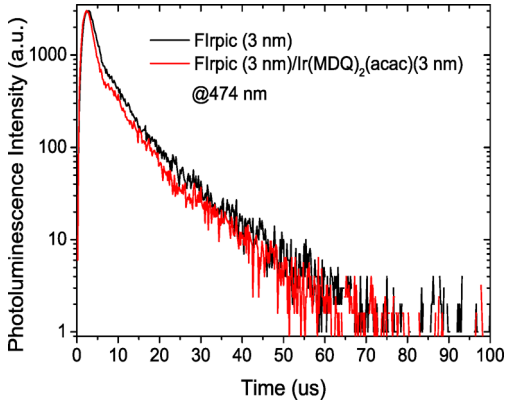

Figure 6. Transient photoluminescence decay curves of the SPPO1:7 wt % FIrpic layer (3 nm) and SPPO1:7 wt % FIrpic (3 nm)/SPPO1:4 wt % $Ir(MDQ)_2(acac)$ (3 nm) layers.

$(MDQ)_2(acac)$ layer. This indicates that there does exist a Förster energy transfer between the red EML and the blue EML.[27] However, the small difference of 0.13 μs between the lifetimes of the two samples (1.6 μs for sample 1 and 1.47 μs for sample 2) shows the Förster energy transfer is minor, which corresponds with the previous conclusion from Figure 5a.

Carrier Trapping. In a host−guest system, electrons and holes are trapped by some guest molecules under an applied electric field in EMLs and then combine directly with the injection carriers, resulting in the emission. The trapping effect usually occurs at a low operation voltage when there is a large energy level difference between the host and guest molecules, leading to the shift of the spectra in a WOLED.[28] From Figure 2a, reducing the hole current by doping $Ir(MDQ)_2(acac)$ into SPPO1 displays that a large number of holes are trapped by $Ir(MDQ)_2(acac)$ molecules. So it is facilitated for the holes on the red guest molecules to combine with the injected electrons from the cathode to emit red light when the red EML is located near the ETL.[29]

Pure and Stable TWOLED and Its Working Principle. According to the results discussed above, we fabricate a TWOLED with the structure of glass/Ag (80 nm)/MoOx (2 nm)/*m*-MTDATA (25 nm)/NPB (15 nm)/TCTA:7 wt % FIrpic (15 nm)/SPPO1:7 wt % FIrpic (4 nm)/SPPO1:4 wt % $Ir(MDQ)_2(acac)$ (11 nm)/BPhen (10 nm)/BPhen:3 wt % Li (20 nm)/Sm (4 nm)/Ag (12 nm)/*m*-MTDATA (40 nm). Here, the thickness of HTL is slightly increased from 10 to 15 nm, and Li is doped into BPhen as the electron guest to reduce the electron injection barrier and to help the electrons to form excitons at the TCTA/SPPO1 interface. Both of the modulations target the enhancement of efficiency and color stability. The curves of current density and luminance with the operating voltage are plotted in the inset of Figure 7a. The current density and luminance reach their maximum values at 12 V. The peak luminance is 15 360 cd/m^2. The device also has a high current efficiency of 13.3 cd/A at 2.22 mA/cm^2, as shown in Figure 7a. It is noted that the device shows pure white CIE coordinates of (0.33, 0.41) and an excellent color stability with a weak color shift of (0.009, 0.001) in the wide luminance range of 10^1−10^4 cd/m^2, which is a rather good chromaticity performance in the TWOLEDs published so far.[5] The normalized spectra of the optimized device at different luminance are presented in Figure 7b, keeping almost unchanged. The inset is the picture of the lighting TWOLED. The optimized TWOLED also exhibits good angle stability, as shown in Figure 7c. Due to the high transmissivity of the semitransparent cathode as shown in the inset of Figure 1, the microcavity effect is relatively low. So the resonance wavelength slightly blue shifts with the increased viewing angle as shown in the inset in Figure 7c, which results in the slight enhancement of the blue emission.

In our device, the utilization of the Li-doped BPhen layer can greatly enhance the electron injection. We made the electron- and hole-only devices with the same EML as the optimized TWOLED. From the current densities in Figure 7d, the electron current is much larger than the hole current, meaning the majority carrier is electron and the recombination zone is mainly determined by the distribution of holes. As shown in Figure 8a, at a low voltage, with the help of the electron guest (Li) and the electron channel ($Ir(MDQ)_2(acac)$), injected electrons hop on SPPO1 molecules and accumulate at the region near the TCTA/SPPO1 interface. However, only few holes can reach the TCTA/SPPO1 interface and further cross the interface to inject the SPPO1 layer due to the high energy barriers and very low hole mobility of SPPO1. So the recombination zone centralizes the interface and is narrow, resulting in the blue emission. Although few excitons diffuse into the red EML, the trapping effect on $Ir(MDQ)_2(acac)$ molecules and the energy transfer from the blue emitter to the red molecules provide the red emission, so a white emission is acquired at a low voltage. With increasing the driving voltage,

dx.doi.org/10.1021/am5006354 | ACS Appl. Mater. Interfaces 2014, 6, 5273−5280

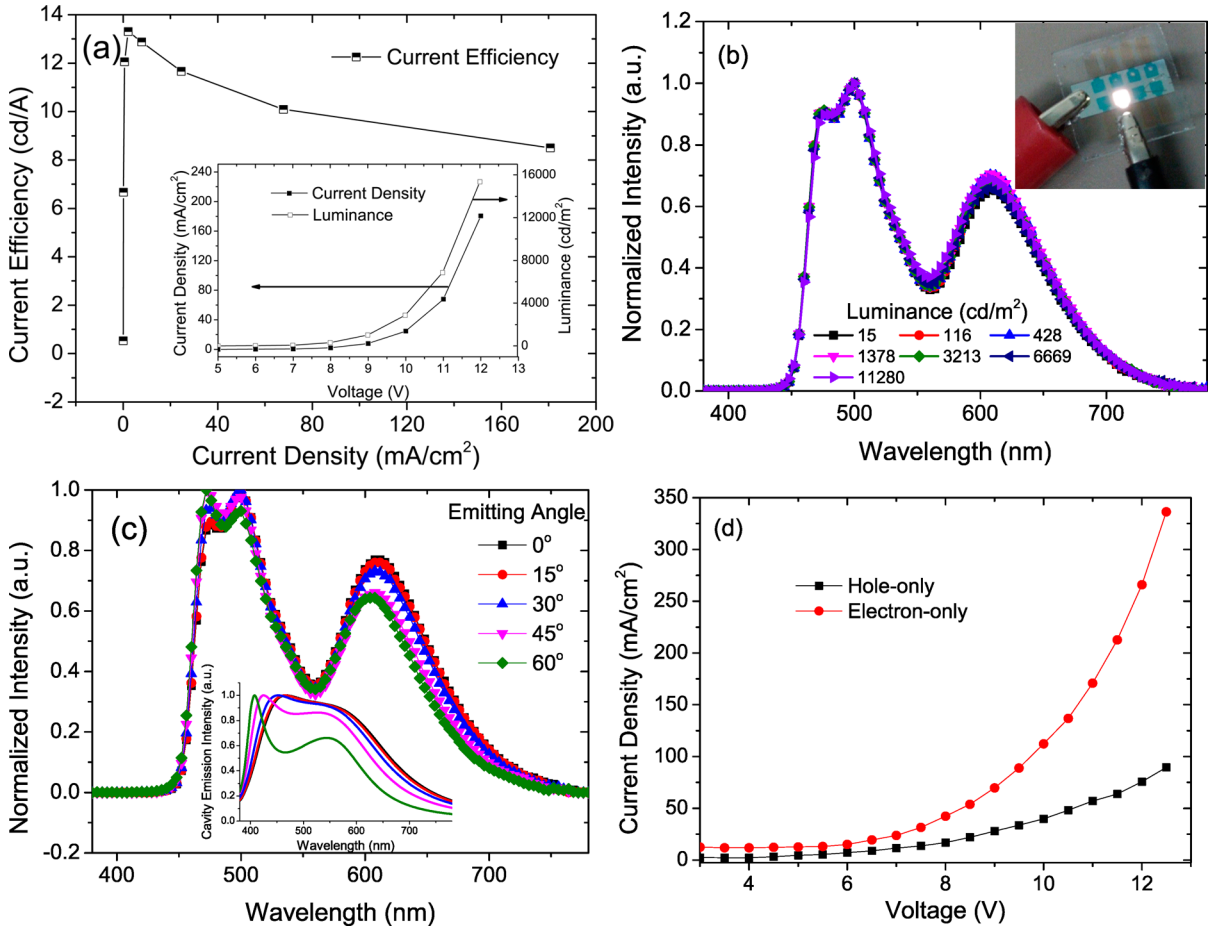

Figure 7. (a) Current efficiency properties in the optimized device. The inset is the current density−luminance−voltage properties. (b) Normalized spectra at the different luminance. The inset is the picture of the lighting device. (c) Spectra at different viewing angles. The inset is the calculated cavity emission spectra. (d) Current densities of the electron- and hole-only devices.

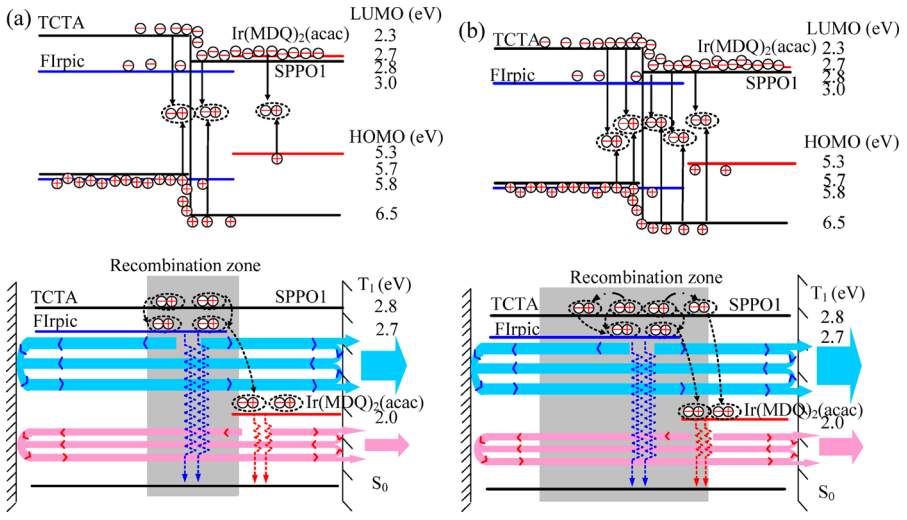

Figure 8. Energy levels and working principle in our TWOLED: (a) is at low voltages and (b) is at high voltages (where the solid arrow is exciton formation, the dash/dotted arrow is exciton diffusion, the dashed arrow is energy transfer, and the thick arrow is light emission).

more holes run across the interface and form excitons on SPPO1 molecules, which widens the recombination zone and greatly enhances the exciton density in the red EML (Figure 8b). The trapping effect is suppressed at a high voltage, while energy transfer from SPPO1 and FIrpic contributes to the red emission. Thus, the TWOLED presents an excellent color stability. Besides, the microcavity effect is an essential fact influencing the chromaticity in a TWOLED. By increasing the transmissivity of the semitransparent cathode and decreasing the distance between the excitons and the reflective anode, the microcavity effect realizes the optical enhancement on the blue emission in our TWOLED, just as discussed in the previous

dx.doi.org/10.1021/am5006354 | ACS Appl. Mater. Interfaces 2014, 6, 5273−5280

section. The enhancement helps to acquire a saturated white light and is independent of the driving voltage, so the microcavity effect also plays an important role in improving both the chromaticity and the stability of the TWOLED.

CONCLUSIONS

In this paper, TWOLEDs based on the dual blue EMLs are designed and discussed. The dual blue EMLs are located near the hole transport layer and the reflective anode to enhance the output of blue emission by utilizing the wide-angle interference, a factor usually ignored in a TOLED. They also possess a heterojunction structure to provide the energy barriers for carriers to control the exciton formation and recombination zone. With the attached carrier channels provided by the guest molecules, more electrons and holes reach the interface of the heterojunction and form excitons, facilitating to acquire the high efficiency in our TWOLED. Both the energy transfer processes between the blue and red phosphor molecules and the trapping effect on the $Ir(MDQ)_2(acac)$ molecules are discussed to improve the color stability of the TWOLED. On the basis of the detailed analysis on the several working processes mentioned above, an optimized TWOLED showing the high efficiency, good chromaticity, and excellent color stability is realized.

AUTHOR INFORMATION

Corresponding Authors

*E-mail: iamsfchen@njupt.edu.cn (S.C.).

*E-mail: wei-huang@njupt.edu.cn/iamdirector@njupt.edu.cn (W.H.).

Present Address

[‖]Electronic Science and Computer Technology, Peking University, Shenzhen 518055, China.

Author Contributions

[§]L.D. and H.S. contributed equally. The manuscript was written through contributions of all authors. All authors have given approval to the final version of the manuscript.

Notes

The authors declare no competing financial interest.

ACKNOWLEDGMENTS

The authors acknowledge financial support from the Ministry of Science and Technology (973 project, Grant No. 2012CB933301), NSFC (Grant Nos. 61274065, 60907047, 51173081, 61136003, BZ2010043, 51172110, and 51372119), the Ministry of Education of China (No. IRT1148), the Research Fund for the Doctoral Program of Higher Education Institutions (Grant No. 20093223120003), the NSF of the Higher Education Institutions of Jiangsu Province (Grant No. 11KJD510003), the Pandeng Project of Nanjing University of Posts and Telecommunications (Grant Nos. NY 210015 and NY211069), the "Qing Lan" Program of Jiangsu Province and Nanjing University of Posts and Telecommunications (Grant No. NY210040), and the Priority Academic Program Development of Jiangsu Higher Education Institutions.

REFERENCES

(1) Kido, J.; Kimura, M.; Nagai, K. Multilayer White Light-Emitting Organic Electroluminescent Device. *Science* **1995**, *267*, 1332−1334.

(2) Chen, Y.; Chen, J.; Ma, D.; Yan, D.; Wang, L. Tandem White Phosphorescent Organic Light-Emitting Diodes Based on Interface-Modified C-60/Pentacene Organic Heterojunction as Charge Generation Layer. *Appl. Phys. Lett.* **2011**, *99*, 103304.

(3) Freitag, P.; Zakhidov, A. A.; Luessem, B.; Zakhidov, A. A.; Leo, K. Lambertian White Top-Emitting Organic Light Emitting Device with Carbon Nanotube Cathode. *J. Appl. Phys.* **2012**, *112*, 114505.

(4) Wang, Q.; Chen, Y.; Chen, J.; Ma, D. White Top-Emitting Organic Light-Emitting Diodes Employing Tandem Structure. *Appl. Phys. Lett.* **2012**, *101*, 133302.

(5) Chen, S.; Wu, Q.; Kong, M.; Zhao, X.; Yu, Z.; Jia, P.; Huang, W. On the Origin of the Shift in Color in White Organic Light-Emitting Diodes. *J. Mater. Chem. C* **2013**, *1*, 3508−3524.

(6) Zhao, Y.; Chen, J.; Ma, D. Ultrathin Nondoped Emissive Layers for Efficient and Simple Monochrome and White Organic Light-Emitting Diodes. *ACS Appl. Mater. Interfaces* **2013**, *5*, 965−971.

(7) Chang, Y.; Song, Y.; Wang, Z.; Helander, M. G.; Qiu, J.; Chai, L.; Liu, Z.; Scholes, G. D.; Lu, Z. Highly Efficient Warm White Organic Light-Emitting Diodes by Triplet Exciton Conversion. *Adv. Funct. Mater.* **2013**, *23*, 705−712.

(8) Xiong, L.; Zhu, W.; Wei, N.; Li, J.; Sun, W.; Wu, X.; Cao, J.; Wang, Z. High Color Rendering Index and Chromatic-Stable White Organic Light Emitting Diodes Incorporating Excimer and Fluorescence Emission. *Org. Electron.* **2013**, *14*, 32−37.

(9) Chang, C. H.; Chen, C. C.; Wu, C. C.; Chang, S. Y.; Hung, J. Y.; Chi, Y. High-Color-Rendering Pure-White Phosphorescent Organic Light-Emitting Devices Employing only two Complementary Colors. *Org. Electron.* **2010**, *11*, 266−272.

(10) Hsu, S. F.; Lee, C. C.; Hwang, S. W.; Chen, C. H. Highly Efficient Top-Emitting White Organic Electroluminescent Devices. *Appl. Phys. Lett.* **2005**, *86*, 253508.

(11) Ji, W.; Zhao, J.; Sun, Z.; Xie, W. High-Color-Rendering Flexible Top-Emitting Warm-White Organic Light Emitting Diode with a Transparent Multilayer Cathode. *Org. Electron.* **2011**, *12*, 1137−1141.

(12) Ji, W.; Zhang, L.; Zhang, T.; Xie, W.; Zhang, H. High-Contrast and High-Efficiency Microcavity Top-Emitting White Organic Light-Emitting Devices. *Org. Electron.* **2010**, *11*, 202−206.

(13) Shao, M.; Guo, X.; Chen, S. F.; Fan, Q. L.; Huang, W. Efficient Top-Emitting White Organic Light Emitting Device with an Extremely Stable Chromaticity and Viewing-Angle. *Chin. Phys. B* **2012**, *21*, 108507.

(14) Freitag, P.; Reineke, S.; Olthof, S.; Furno, M.; Lussem, B.; Leo, K. White Top-Emitting Organic Light-Emitting Diodes with Forward Directed Emission and High Color Quality. *Org. Electron.* **2010**, *11*, 1676−1682.

(15) Chen, S. F.; Shao, M.; Guo, X.; Qian, Y.; Shi, N. E.; Xie, L. H.; Yang, Y.; Huang, W. Top-Emitting White Organic Light-Emitting Diodes Based on a ZnS Light Outcoupling Layer. *Acta Phys. Sin.* **2012**, *61*, 087801.

(16) Chen, S.; Kwok, H.-S. Alleviate Microcavity Effects in Top-Emitting White Organic Light-Emitting Diodes for Achieving Broadband and High Color Rendition Emission Spectra. *Org. Electron.* **2011**, *12*, 2065−2070.

(17) Thomschke, M.; Reineke, S.; Lussem, B.; Leo, K. Highly Efficient White Top-Emitting Organic Light-Emitting Diodes Comprising Laminated Microlens Films. *Nano Lett.* **2012**, *12*, 424−428.

(18) Dodabalapur, A.; Rothberg, L. J.; Jordan, R. H.; Miller, T. M.; Slusher, R. E.; Philips, J. M. Physics and Applications of Organic Microcavity Light Emitting Diodes. *J. Appl. Phys.* **1996**, *80*, 6954−6965.

(19) Xie, J.; Chen, C.; Chen, S. Blue Top-Emitting Organic Light-Emitting Devices Based on Wide-Angle Interference Enhancement and Suppression of Multiple-Beam Interference. *Org. Electron.* **2011**, *12*, 322−328.

(20) So, S. K.; Choi, W. K.; Leung, L. M.; Neyts, K. Interference Effects in Bilayer Organic Light-Emitting Diodes. *Appl. Phys. Lett.* **1999**, *74*, 1939−1941.

(21) Deng, L.; Chen, S.; Xie, J.; Qian, Y.; Xie, L.; Shi, N.; Liu, B.; Huang, W. Color-Saturated and Angle-Stable Blue Top-Emitting

Organic Light-Emitting Diodes Based on Semitransparent Bilayer Cathode: Theory and Experiment. *Org. Electron.* **2013**, *14*, 423−429.
(22) Weichsel, C.; Reineke, S.; Furno, M.; Lussem, B.; Leo, K. Organic Light-Emitting Diodes for Lighting: High Color Quality by Controlling Energy Transfer Processes in Host-Guest-Systems. *J. Appl. Phys.* **2012**, *111*, 033102.
(23) Lan, Y. H.; Hsiao, C. H.; Lee, P. Y.; Bai, Y. C.; Lee, C. C.; Yang, C. C.; Leung, M. K.; Wei, M. K.; Chiu, T. L.; Lee, J. H. Dopant Effects in Phosphorescent White Organic Light-Emitting Device with Double-Emitting Layer. *Org. Electron.* **2011**, *12*, 756−765.
(24) Bilovic, V.; Khalfin, V. B.; Gu, G.; Burrows, P. E.; Garbuzov, D. Z.; Forrest, S. R. Weak Microcavity Effects in Organic Light-Emitting Devices. *Phys. Rev. B* **1998**, *58*, 3730−3740.
(25) Al Attar, H. A.; Monkman, A. P.; Tavasli, M.; Bettington, S.; Bryce, M. R. White Polymeric Light-Emitting Diode Based on a Fluorene Polymer/Ir Complex Blend System. *Appl. Phys. Lett.* **2005**, *86*, 121101.
(26) Li, Y. Q.; Rizzo, A.; Mazzeo, M.; Carbone, L.; Manna, L.; Cingolani, R.; Gigli, G. White Organic Light-Emitting Devices with CdSe/ZnS Quantum Dots as a Red Emitter. *J. Appl. Phys.* **2005**, *97*, 113501.
(27) Zhao, Y. B.; Zhu, L. P.; Chen, J. S.; Ma, D. G. Improving Color Stability of Blue/Orange Complementary White OLEDs by Using Single-Host Double-Emissive Layer Structure: Comprehensive Experimental Investigation into the Device Working Mechanism. *Org. Electron.* **2012**, *13*, 1340−1348.
(28) Zhao, F.; Zhang, Z.; Liu, Y.; Dai, Y.; Chen, J.; Ma, D. A Hybrid White Organic Light-Emitting Diode with Stable Color and Reduced Efficiency Roll-Off by Using a Bipolar Charge Carrier Switch. *Org. Electron.* **2012**, *13*, 1049−1055.
(29) Pearson, C.; Cadd, D. H.; Petty, M. C.; Hua, Y. L. Effect of Dye Concentrations in Blended-Layer White Organic Light-Emitting Devices Based on Phosphorescent Dyes. *J. Appl. Phys.* **2009**, *106*, 064516.